Journal of the European Ceramic Society 19 (1999) 1299–1306

PII: S0955-2219(98)00424-5
0955-2219/99/$ - see front matter

Influence of the Electric Field on Vickers Indentation Crack Growth in $BaTiO_3$

G. A. Schneider* and V. Heyer

Technische Universität Hamburg-Harburg, Advanced Ceramics Group, D-21073 Hamburg, Germany

Abstract

In this study, the Vickers indentation method was used to determine the crack growth of ferroelectric barium titanate ($BaTiO_3$) ceramic under the influence of electric fields. It was verified that an applied electric field induces distinct anisotropic crack growth parallel and perpendicular to the poling direction which is mainly interpreted as an anisotropy in fracture toughness. The curve of the measured crack lengths as a function of the applied electric field shows similarity with the strain hysteresis. Curves of cracks parallel and perpendicular to the electric field direction are symmetric to each other. Stress-induced ferroelastic domain switching is used to explain the observed crack lengths anisotropy and change in fracture toughness. © *1999 Elsevier Science Limited. All rights reserved*

Keywords: $BaTiO_3$ and titanates, ferroelectric properties, toughness and toughening.

1 Introduction

Ferroelectric ceramics are used in large quantities in a variety of applications in which they are not mechanically stressed to a significant extend. Because of their fast response times and precise displacement control they are very suitable for replacing conventional mechanical and electromechanical devices in actuating systems. However, the main disadvantage is their brittleness. They tend to develop critical crack growth due to mechanical and electrical loads and are therefore susceptible to fracture. The mechanically related problems most common in ferroelectric ceramics arise from internal stresses generated by phase transitions and reorientation of ferroelectric domains when they are subjected to external loads. In this respect electric fields might deteriorate the mechanical properties of the material. Accordingly, understanding the fracture behaviour of ferroelectric ceramics is the key to improve reliability and assess lifetime of piezoelectric devices.

Analyses which are capable of describing stress relaxation due to ferroelastic domain switching as well as stress distribution and crack propagation phenomena at the tip of an elliptical radial crack produced by Vickers or Knoop indentation have been performed by several researchers.[1–8] Especially the Vickers indentation test technique[9–12] under an additionally applied static electric field is widely used for the fracture toughness analysis in poled ferroelectric ceramics. The main measured effect of the induced electric polarization in the ferroelectric material is an anisotropic crack growth parallel and perpendicular to the poling direction. The evaluation of the experimental data with the known concepts of fracture mechanics leads to the conclusion of an anisotropy in fracture toughness as a material property of ferroelectric ceramics. The anisotropy in the fracture toughness is induced by energy dissipating ferroelastic domain switching during crack growth due to the mechanical stress field in the vicinity of the crack tip.[2–6] The tensile stresses acting normal to the crack plane induce ferroelastic reorientation of these domains which are aligned mostly parallel to the crack. This effect leads to pronounced R-curves which was shown at compact-tension specimens made of barium titanate.[13,14] Controlled crack growth was induced in unpoled and poled samples as well as under an additionally applied electric D.C. field and the toughening was explained with the development of a ferroelastic switching zone around the crack. The applied electric field parallel to the crack front increases the initial fracture toughness and results in a stronger R-curve behaviour.

Guiu *et al.*[7] suggest another explanation for the anisotropy in the fracture toughness of Vickers indentation cracks. It is argued that the plastic

*To whom correspondence should be addressed. Fax: + 49-40-42878-2647; e-mail: g.schneider@tu-harburg.de

deformation stress field produced beneath the Vickers indentation is anisotropic, having higher intensity, or being longer range, in the direction normal to poling. The anisotropy in the plastic deformation field can be induced by the preferred orientation of the ferroelectric domains in the polarised material and differences in the shear moduli c_{44} and c_{66}.

Ferroelectric ceramics undergo residual stresses associated with the phase transition that occurs on cooling through the Curie temperature. These internal stresses vary in magnitude dependent on the transformation strain and the elastic modulus. Dependent on grain size these stresses can produce microcracks and spontaneous cracking.[15] Not only electrically induced polarization in the ferroelectric ceramic also applied electric fields directly interact with existing cracks. The difference in the dielectric permittivity between the ceramic and the crack filling medium determines the character of the electric field effect which can enhance or hinder crack growth.[16–20]

In this study the crack growth in a $BaTiO_3$ ceramic was investigated under applied electric fields up to 4 times the coercive field strength by using the Vickers indentation technique. The change in crack length and fracture toughness in connection with the influence of polarization switching on the crack generating stresses as well as crack tip switching processes is qualitatively discussed.

2 Experimental and Results

2.1 Preparation of the bulk material

Samples were prepared from a commercially available $BaTiO_3$ powder, namely Alpha 99% 2 μm (Johnson & Matthey GmbH Karlsruhe, Germany) with a $BaO + SrO\text{-}TiO_2$ ratio of 0·987. The bulk material was fabricated in three steps. In the first two steps the specimens were formed by pressing: (1) uniaxial forming pressure of 29 MPa, (2) isostatic forming pressure of 750 MPa. Then the pressed powder was sintered in air at 1250°C for 3 h to a final relative density of 95·4% of the theoretical density $\rho = 6{\cdot}017\ \mathrm{g\,cm^{-3}}$. The specimens had an average grain size of 10 μm and a tetragonal crystal structure at room temperature. After polishing with diamond paste the beam specimens have dimensions of $3\times3\times38$ mm. Silver paint was used as electrodes which were applied on two planparallel and opposite surfaces.

2.2 Young's modulus and Poisson ratio

The Young's modulus of poled specimens was determined applying the pulse-echo method with the Universal Ultrasonic Flaw Detector USM 3 (Krautkrämer-Branson GmbH, Germany). A transversal and longitudinal ultrasonic pulse with a frequency spectrum between 10 and 15 MHz was sent parallel and perpendicular to the poling direction in the specimen to measure the speed of sound. From the results the Young's modulus $Y = 88$ GPa and the Poisson number $\nu = 0{\cdot}35$ were determined neglecting the small elastic anisotropy of the material.

2.3 Polarisation and strain hysteresis

In order to characterise the ferroelectric properties of barium titanate the polarization P and the strain γ were measured as a function of the applied electric field E. For the polarization measurement a Sawyer–Tower circuit was used. In the circuit a big capacity is connected in series to the specimen so that by varying the electric field the electric charge at specimen's electrodes can be determined. Figure 1 shows the measured polarization hysteresis. The strain parallel to the electric field direction (butterfly loop) was measured via an inductive system (Fig. 2).

2.4 Crack growth by Vickers indentation and fracture toughness under electric field

For isotropic, homogeneous materials, explicit equations for the radial crack evolution by a sharp indenter have been empirically formulated.[9] The critical stress intensity factor or fracture toughness K_{Ic} can be expressed in terms of material constants, indentation load and indentation induced crack length such as

$$K_{Ic} = 0{\cdot}032 \cdot H \cdot \sqrt{c}\sqrt{\frac{Y}{H}} \cdot \left(\frac{a}{c}\right)^{-3/2},\ H = \frac{P}{2 \cdot c^2} \qquad (1)$$

where P is the applied indentation load, Y is the Young's modulus, $2c$ is the Vickers diagonal, a is the crack half length and H is the Vickers hardness. The factor 0·032 was chosen on the basis of Ref. 9 because the fracture toughness values of unpoled specimens are in good agreement with the results of other test methods and the typical half penny crack shape was found in the tested specimens.

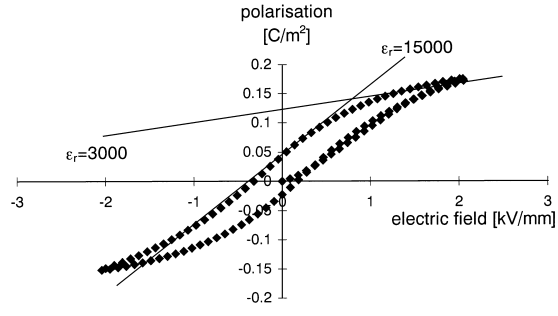

Fig. 1. Polarization hysteresis of the used $BaTiO_3$ ceramic.

A commercial Vickers indentation facility (Zwick 3212, Zwick, Germany) was used. Tests were performed in a silicon oil tub to prevent subcritical crack growth and electric discharge through air. The peak indentation load of 40 N was applied for 10 s, then, unloaded rapidly. To generate electric fields, a power supply for voltages up to 12·5 kV/D.C. was used. Before testing the specimens were poled by an electric field of $E = 1\ \mathrm{kV\,mm^{-1}}$. Indentation tests were conducted during the action of various electric fields both in poling (positive) and opposite to the poling direction (negative) to investigate the effect of electric polarisation on crack growth (Fig. 3). Twenty-five indentations were performed and radial crack lengths parallel, a_{II}, and perpendicular, $a_{\perp}$, to the electric field direction were measured with an optical microscope immediately after indentation for each electric field level (Fig. 4). Figure 5 shows a typical crack system. It is noted that there is the well known crack lengths anisotropy. As can be seen also side cracks may develop which are probably due to the strong internal stresses. Nevertheless the large number of data points should minimise the experimental error connected with side cracks. It is in any case evident that crack growth perpendicular to the poling direction is significantly greater than in the parallel direction.

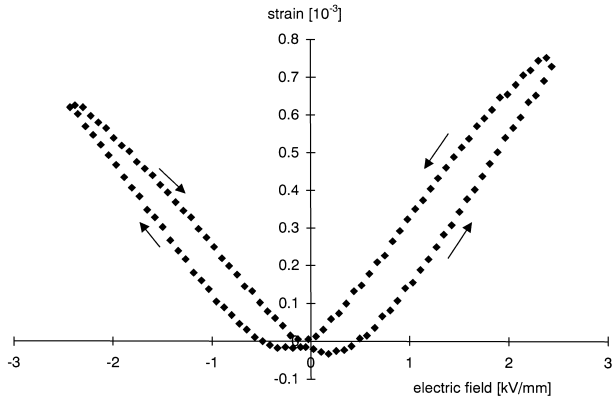

Fig. 2. Strain hysteresis of the used $BaTiO_3$ ceramic.

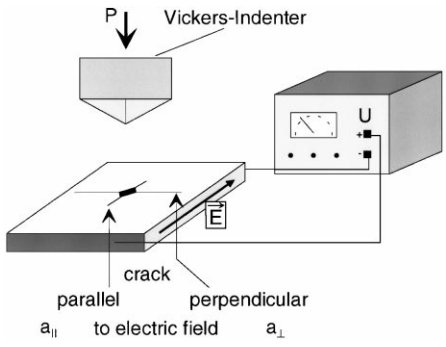

Fig. 3. Experimental set-up.

Table 1 lists the variation in crack lengths along with different electric fields and their standard deviations. From the crack lengths the fracture toughness was calculated according to eqn (1). The results are summarised in Table 2.

3 Discussion

3.1 Electric field around indent

In order to discuss the influence of the applied electric field on the development of the crack system around the indent the electric field distribution, $\vec{E}(\vec{r})$, in the vicinity of the indent must be known. As a rough estimation the indent is approximated by a spherical void of radius c. The applied electric field, $\vec{E}_0$, produces a polarisation, $\vec{P}$,[21,22]

$$\vec{P} = \frac{(\varepsilon_r - 1)\varepsilon_0}{1 + \frac{\varepsilon_r - 1}{3}} \vec{E}_0 \cong 3\varepsilon_0 \vec{E}_0 \text{ for } \varepsilon_r \gg 1 \qquad (2)$$

which produces an electric far field $\vec{E}_P$

$$\vec{E}_P(\vec{r}) = \frac{3(\vec{P}\cdot\vec{r})\cdot\vec{r} - r^2\cdot\vec{P}}{4\cdot\pi\cdot\varepsilon_0\cdot r^5} \qquad (3)$$

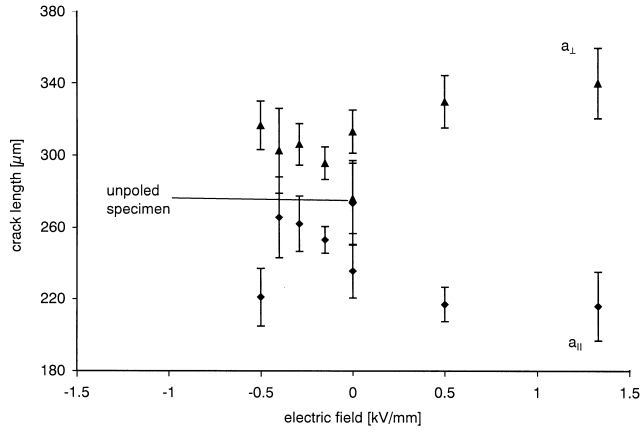

Fig. 4. Measured crack lengths via the applied electric field parallel (a_{II}) and perpendicular ($a_{\perp}$) to the field direction.

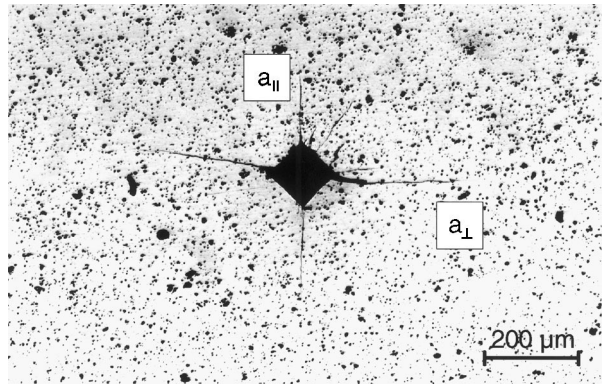

Fig. 5. Dimensions of indentation induced cracks.

Table 1. Measured crack lengths parallel (a_{II}) and perpendicular ($a_\perp$) to the applied electric field; $\bar{a}$: mean value, δa: standard deviation

Specimen	E*(kV mm^{-1})*	$a_{II} \pm \delta a$*(μm)*	$a_\perp \pm \delta a$*(μm)*
Poled	+1·33	216 ± 19	339·5 ± 19·5
Poled	+0·5	217 ± 9·5	329·5 ± 15·5
Poled	0	235·5 ± 15	313 ± 12
Unpoled	0	273·5 ± 23·5	276 ± 19·5
Poled	−0·15	253 ± 7·5	295·5 ± 9
Poled	−0·29	262 ± 15·5	306 ± 11·5
Poled	−0·4	265·5 ± 22·5	302·5 ± 23·5
Poled	−0·5	221 ± 16	316·5 ± 13·5

Table 2. Fracture toughness parallel $K_{Ic,II}$ and perpendicular $K_{Ic,\perp}$ to the electric field

Specimen	E*(kV mm^{-1})*	$K_{Ic,II}$*(MPa$\sqrt{m}$)*	$K_{Ic,\perp}$*(MPa$\sqrt{m}$)*
Poled	+1·33	1·63 ± 0·11	0·83 ± 0·03
poled	+0·5	1·62 ± 0·05	0·86 ± 0·03
Poled	0	1·43 ± 0	070·93 ± 0·03
Unpoled	0	1·14 ± 0	071·13 ± 006
Poled	−0·15	1·28 ± 0·03	1·02 ± 002
Poled	−0·29	1·59 ± 0·05	1·03 ± 0·03
Poled	−0·4	1·19 ± 0·07	0·98 ± 0·06
Poled	−0·5	1·57 ± 0·08	0·92 ± 0·03

In these equations, ε_r, denotes the relative permittivity of the material and ε_0 is the vacuum permittivity. The total electric field, $\vec{E}$, around the indent is the superposition of the applied electric field and the electric dipole field. For an applied electric field in z-direction this leads for $r > c$ to:

$$E_x = \frac{\varepsilon_r - 1}{2 \cdot \varepsilon_r + 1} \cdot E_0 \cdot \left(\frac{c}{r}\right)^3 3 \cdot \sin(\theta)\cos(\theta) = E_y \quad (4)$$

$$E_z = E_0 - \frac{\varepsilon_r - 1}{2 \cdot \varepsilon_r + 1} \cdot E_0 \cdot \left(\frac{c}{r}\right)^3 (3 \cdot \cos^2(\theta) - 1) \quad (5)$$

In x, y and z direction i.e. $\theta = 90°$ or $0°$, respectively, the x and y components of the electric field are zero. The electric field in z direction at the surface of the sphere ($r = c$) for $\theta = 0°$ vanishes whereas for $\theta = 90°$ it is intensified by a factor of 1·5 because the dipole field is directed in negative z direction. Hence the local electric field around the indent deviates significantly from the applied electric field for $r \cong c$ but for $r > 2c$ the effect of the indent (sphere) is small and may be neglected.

3.2 Median cracks

As described in Ref. 11 subsurface median cracks induced by elastic/plastic contact through a Vickers indentation with opening angle 2Ψ develop during the loading half cycle. In this regime both the residual stresses due to the plastic deformation, σ_r,

$$\sigma_r \approx Y\left(\frac{a}{b}\right)^3 \cot(\Psi)\left(\frac{c}{r}\right)^3 \quad (6)$$

and the subsurface elastic contact stresses σ_e

$$\sigma_e = g(\Phi) H \frac{\alpha_0}{\pi}\left(\frac{c}{r}\right)^2 \quad (7)$$

are tensile and perpendicular to the median planes containing the load axes. b describes the dimension of the plastic zone, α_0 is a geometrical constant being π for a circular contact. $g(\Phi)$ is an angular function $\approx 0{\cdot}1$ being negative for $\Phi = 0°$ at the surface (compressive stresses) and positive for $\Phi = 90°$ (perpendicular to the surface, tensile stresses).

If these tensile stresses exceed the coercive stress, σ_{coercive} ferroelastic domain switching occurs and relaxes the tensile stresses. For the used $BaTiO_3$ ceramic, ferroelastic behaviour in bending occurs between 20 and 60 MPa (A. Kolleck, pers. comm.) resulting in an average coercive stress $\bar{\sigma}_{\text{coercive}} = 40$ MPa. Introducing this value into eqns (6) and (7) gives the radius R around the Vickers indentation where domain switching occurs: $R_e = 220\,\mu$m and $R_r = 270\,\mu$m for $\Psi = 68°$ and $b/a = 1{\cdot}02$.

An applied electric field of 1·5 kV mm^{-1} increases the coercive stress by approx. 25% (Kolleck, pers. comm.) which reduces switching to $R_e = 196\,\mu$m and $R_r = 250\,\mu$m. These radii are of the order of the measured crack lengths (see Table 1 and Table 2).

The elastic stress field develops instantaneously when the tip of the indent touches the surface of the ceramic. Therefore the elastic stress field is present before the median cracks develop and domain switching due to this stress field occurs. Median cracks develop after a certain plastic deformation is produced. Therefore the residual stress field arises simultaneously with crack initiation and growth and will probably not be relaxed due to domain switching.

If the material is unpoled domain switching due to the elastic stress field will be isotropic and also the stress relaxation will be axial symmetric around the Vickers indent. If an electric field is applied parallel to one of the diagonals of the Vickers indent the situation changes as follows: The polarisation vectors of the domains are oriented mostly parallel to the applied electric field. Ferroelastic domain switching due to the tensile stresses σ_e takes place during the loading half cycle below the indent. But this domain switching is concentrated on the area which is parallel to the electric field because only there the tensile stresses are oriented perpendicular to the electric field (Fig. 6). Accordingly stress relaxation occurs mainly in the direction parallel to the electric field and the driving

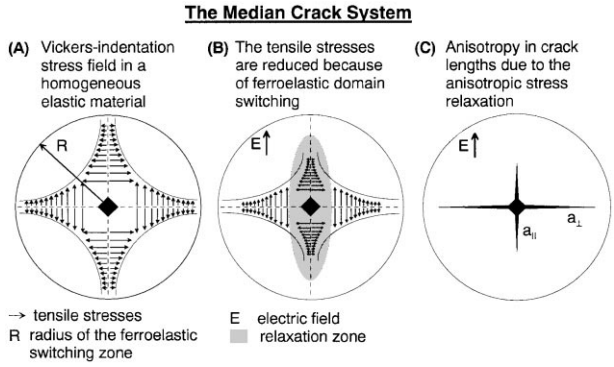

Fig. 6. Model of tensile stress relaxation due to ferroelastic domain switching in the material.

force for the median crack parallel to the electric field decreases. As a consequence the crossed median cracks are expected to have different extension being longer in direction perpendicular to the electric field than in parallel direction.

In addition stronger electric fields have a stronger poling effect which means that more domains can be switched ferroelastically by the elastic stress field. Therefore stress relaxation will increase in direction parallel to the electric field and decrease in orthogonal direction and the corresponding crack lengths will decrease and increase, respectively.

3.3 Radial cracks

The development of the radial cracks occurs during the unloading half cycle.[10–12] During the loading half-cycle the elastic contact hoop stresses are compressive at the surface and compensate the tensile residual hoop stresses. Along with the unloading the elastic contact stresses disappear and only the residual stresses from the plastic deformation remain. These residual hoop stresses are tensile and the corresponding radial stresses are compressive. As shown above these residual stresses are strong enough to induce ferroelastic switching up to a radius $R_r \approx 250\ \mu$m. Therefore also for the radial cracks stress relaxation could take place leading to an anisotropic residual stress field on the surface with the same effect as already described for the median cracks. On the other hand stable crack growth will occur simultaneously to the unloading half cycle and it is not clear if stress relaxation of the residual stress field arises fast enough.

3.4 Crack tip domain switching

The above described relaxation model especially for median cracks is an alternative approach in comparison to the crack tip domain switching models.[2–6] The basic idea of the crack tip switching models is that the high tensile stresses at the crack tip perpendicular to the crack path lead to a local polarization change. If the coercive stress, σ_{coercive}, is exceeded near the crack tip, domains originally oriented mainly parallel to the crack change their polarization by 90° switching due to these tensile stresses. Accompanied with the polarization change is a strain mismatch $\Delta\varepsilon_{\text{switch}}$ because of the tetragonal crystal structure of the $BaTiO_3$. The c axis is about 1% longer than the a axis. Therefore the material expands locally around the crack tip in orthogonal direction and it shrinks parallel to the crack direction. No volume change occurs because domain switching is a shear process. Compressive stresses normal to the crack ligaments would be present without a crack and are relaxed by the existing crack leading to crack tip shielding during crack advance. The toughness increase, ΔG_{Ic}, due to this shielding can be expressed by the energy density $\sigma_{\text{coercive}}\Delta\varepsilon_{\text{switch}}$ times the width of the switching zone, $2h$,

$$G_{Ic} = G_0 + \Delta G_{Ic} = G_0 + 2h\sigma_{\text{coercive}}\Delta\varepsilon_{\text{switch}} \tag{8}$$

G_0 denotes the toughness in the absence of domain switching. The zone half width h is determined from the crack tip stress field

$$h = A\left(\frac{K_{Ic}}{\sigma_{\text{coercive}}}\right)^2 \tag{9}$$

A is a constant depending on the zone shape which is related to the used switching criterion which is a matter of research. With

$$G_{Ic} = \frac{K_{Ic}^2}{Y\cdot(1-\nu^2)}\ \text{(plane strain)} \tag{10}$$

we get[23]

$$G_{Ic} = \frac{G_0}{1 - 2A\frac{\Delta\varepsilon_{\text{switch}}Y(1-\nu^2)}{\sigma_{\text{coercive}}}} \tag{11}$$

Equation (11) is identical with $\Delta K = \sqrt{A}Y(1-\nu^2)\Delta\varepsilon_{\text{switch}}\sqrt{h}$ for small $\Delta\varepsilon_{\text{switch}}$.[24]

The influence of an electric field on toughening is twofold:

- It changes the number of switchable domains by the stress field at the crack tip. Therefore the strain mismatch $\Delta\varepsilon_{\text{switch}}$ changes.
- The coercive stress σ_{coercive} necessary to switch the domains is changed.

It is clear that for tensile stresses of 'parallel' cracks σ_{coercive} increases because the electric field 'holds' the polarization. For cracks perpendicular to the electric field the effect is just the opposite. The

experimental result shows a distinct toughness increase for cracks oriented parallel to the electric field and a decrease for cracks oriented perpendicular to it. According to eqn (11) this can only be understood when the relative changes of the switching strains due to the electric field are stronger than the relative changes of the coercive stress. It is very probable that the growth of median cracks to radial cracks during unloading is strongly determined by the crack tip domain switching processes.

3.5 Similarity between butterfly loop and crack lengths as a function of the electric field

It is especially interesting to discuss the effect of a negative electric field applied in direction opposite to poling. If this negative electric field is increased up to $-0{\cdot}4\ \mathrm{kV\,mm^{-1}}$ the crack lengths a_{II} and $a_{\perp}$, increase and decrease, respectively. For higher negative electric fields the effect is reversed. This can be understood as follows: The number of switchable domains dominates both the relaxation of the elastic or residual stress field before the crack enters into these stress fields and the crack tip switching processes. The number of switchable domains is proportional to the strain hysteresis (butterfly) loop. It is clear that the number of switchable domains for 'parallel' cracks has a minimum corresponding to a maximum crack length at the (negative) coercive field. The opposite is valid for 'perpendicular' cracks leading to a minimum in crack length. In addition a direction can be assigned to the crack lengths measurements. It starts with poled specimens of $1\ \mathrm{kV\,mm^{-1}}$. The electric field is decreased and reversed to negative fields. At the coercive field the sample changes the poling direction. This effect can be clearly seen in the crack lengths curves. Therefore by reflecting the measured crack lengths at the ordinate, $E = 0\ \mathrm{kV\,mm^{-1}}$,—as a consequence we double our data points—a crack lengths hysteresis loop can be constructed similar to the strain hysteresis loop (Fig. 7). The same happens for the calculated fracture toughness curves (Fig. 8).

Of course, these crack lengths loops and K_{Ic} butterfly loops are not measured with a continuously varying electric field. The measurement is performed in discrete steps as described before. As a consequence some hysteresis effects enter, but they are small for our $BaTiO_3$. Also the maxima and minima of the crack lengths do not exactly occur at the coercive field. This is assigned to the electric field perturbance due to the Vickers indent as well as the existing median cracks. The Vickers indent intensifies the electric field for 'perpendicular' cracks and diminishes it for 'parallel' cracks. Therefore we expect that we need higher applied electric fields to reach locally the coercive field for

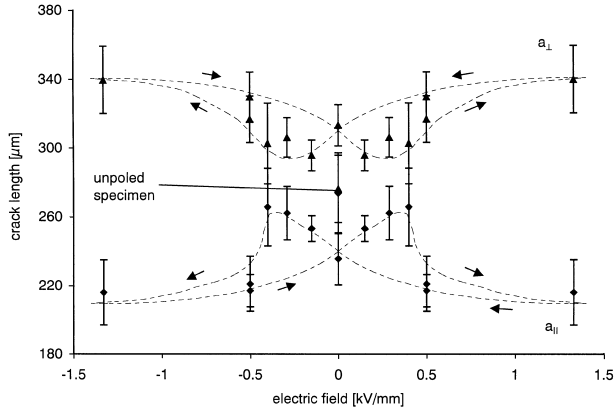

Fig. 7. Measured crack lengths parallel (a_{II}) and perpendicular ($a_{\perp}$) to the applied electric field.

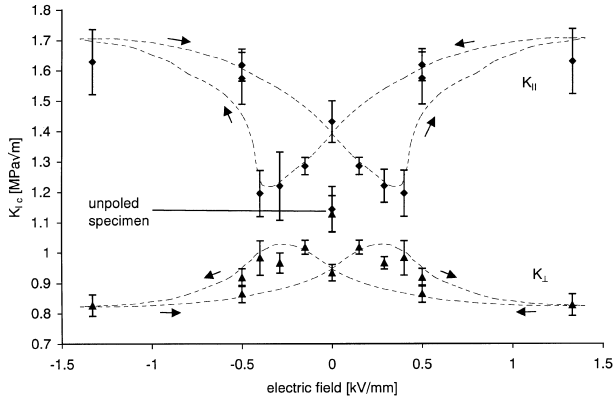

Fig. 8. Calculated fracture toughness with constant Vickers hardness H parallel $K_{Ic,II}$ and perpendicular $K_{Ic,\perp}$ to the electric field.

parallel cracks and the opposite for 'perpendicular' cracks which is in qualitative agreement with the measurements (see Fig. 7). Having these effects in mind the similarity between the strain hysteresis loop and crack lengths loop is surprisingly good.

3.6 'Impermeable' cracks

Suo[16] proposed that in dielectrics remotely applied electric fields E_0 perpendicular to a so–called impermeable crack—that is with zero electric displacement, D, inside the crack perpendicular to the crack surface—lead to singular electric displacement fields around the crack tip

$$D(r) \propto \frac{K_{IV}}{\sqrt{2\pi r}} \tag{12}$$

with the so-called field intensity factor K_{IV}

$$K_{IV} = \varepsilon_0 \varepsilon_r E_0 \sqrt{\pi a} \tag{13}$$

The electrical energy release rate G_{IV} which is connected with the field intensity factor is

$$G_{IV} = -\frac{K_{IV}^2}{2\varepsilon_r \varepsilon_0} \tag{14}$$

It is interesting to recognise that G_{IV} is always negative. This electric field concentration does not occur for cracks oriented parallel to the applied electric field. The consequence for the performed Vickers experiments should be that cracks perpendicular to the applied electric field would 'feel' an additional negative electric crack driving force, G_{IV}, which should reduce crack growth. This contradicts the experimental finding that just $a_\perp$ is always longer than a_{II}. At least this effect must be small. On the other hand a simple calculation for the Vickers cracks gives $G_{IV} = -33\ \mathrm{J\,m^{-2}}$ ($a = 350\,\mu\mathrm{m}$, $\varepsilon_r = 3000$, $\mathrm{E} = 1{\cdot}5\ \mathrm{kV\,mm^{-1}}$). According to eqn (10) the measured K_{Ic} values for cracks perpendicular to the electric field correspond to a critical energy release rate between 2 and 3 $\mathrm{J\,m^{-2}}$. Therefore the effect of the electric energy release rate should exceed the domain switching effect by far. It should be the dominant effect. This dielectric result will be changed only slightly for $BaTiO_3$ with a weak piezoelectric coupling. The strong discrepancy is most probably due to the necessary condition[16,17] that

$$\frac{\varepsilon_f}{\varepsilon_r} \ll \frac{b}{a} \tag{15}$$

where b is the maximum crack opening in the middle of a Griffith crack and ε_f the relative permittivity of the medium inside the crack. In order to check the applicability of K_{IV}, we assume that the ellipticity of the crack comes from an external applied stress σ_y^0 perpendicular to the crack plane and the material behaves ideally dielectric without any piezoelectric or electrostrictive coupling between mechanical and electrical fields. The crack opening u is given by

$$u(x) = \frac{\sigma_y^0}{Y}\sqrt{a^2 - x^2} \tag{16}$$

for $-a < x < a$.

Introducing the mode stress intensity factor, K_I, given by

$$K_I = \sigma_y^0 \sqrt{\pi a} \tag{17}$$

the crack opening at $x = 0$ which equals b may be written as:

$$u(0) = \frac{K_I}{Y}\sqrt{\frac{a}{\pi}} = b \tag{18}$$

With eqn (18) it is possible to check the inequality of eqn (15). The highest possible value for b is given when the fracture toughness, K_{Ic}, of the ceramic material is reached. Therefore using eqn (18) we rewrite the inequality eqn (15) as follows:

$$\frac{\varepsilon_f}{\varepsilon_r}\frac{Y\sqrt{\pi a}}{K_{Ic}} \ll 1 \tag{19}$$

Using the values of the investigated $BaTiO_3$, $\varepsilon_r = 3000$, $\varepsilon_f = 1$, $Y = 88\,\mathrm{GPa}$, $a = 350\,\mu\mathrm{m}$, $K_{Ic} = 1\,\mathrm{MPa}\sqrt{\mathrm{m}}$ we get

$$\frac{\varepsilon_f}{\varepsilon_r}\frac{Y\sqrt{\pi a}}{K_{Ic}} \approx 0{\cdot}9 \tag{20}$$

As 0·9 is not much smaller than 1 it excludes applying to K_{IV}. This result shows clearly that it is physically questionable to apply the impermeable crack approach and that the corresponding negative energy release rate is strongly overestimated. Additionally it is shown that due to the small opening displacement the crack is permeable for the electric field. As a consequence electric field singularities as predicted by eqn (12) which would strongly influence the crack tip switching processes are overestimated.

4 Conclusions

The Vickers indentation technique was used to determine the influence of an electric field on crack growth in $BaTiO_3$. A distinct electric field dependence of the crack lengths could be detected. Cracks perpendicular to the electric field are always longer than cracks parallel to it. Using negative electric fields it could be shown that approx. at the coercive field a_{II} and $a_\perp$ are closest to each other being near the isotropic crack lengths of the unpoled specimens. In addition a crack lengths hysteresis loop similar to the strain hysteresis loop was introduced. This similarity is a strong hint that mostly the strain mismatch during ferroelastic switching which is proportional to the strain hysteresis dominates the relaxation. This result is valid both for crack tip switching processes and stress relaxation of the elastic or residual Vickers indentation stress field. The discussion of K_{IV} shows that the corresponding negative energy release rate is overestimated which can be explained by the problematic assumption that the crack interior has zero permittivity. It could be also shown that the electric field disturbance of the Vickers pyramid is small.

Acknowledgements

The authors gratefully acknowledge support by the German Science Foundation (DFG).

References

1. Esakul, K. A., Gerberich, W. W. and Koepke, B. G., Stress relaxation in PZT. *J. Am. Ceram. Soc.*, 1980, **63**(1,2), 25–30.
2. Mehta, K. and Virkar, A. V., Fracture mechanics in ferroelectric–ferroelastic lead zirconate titanate (Zr:Ti = 0·54: 0·46) ceramics. *J. Am. Ceram. Soc.*, 1990, **73**(3), 567–574.
3. Pisarenko, G. G., Chushko, V. M. and Kovalev, S. P., Anisotropy of fracture toughness in piezoelectric ceramics. *J. Am. Ceram. Soc.*, 1985, **68**(5), 259–265.
4. Tobin, A. G. and Pak, Y. E., Effect of electric fields on the fracture behaviour of PZT ceramics. *Proc. SPIE*, 1993, **1916/79**, 78–86.
5. Okazaki, K., Mechanical behaviour of ferroelectric ceramics. *Bull. Am. Ceram. Soc.*, 1984, **63**(9), 1150–1152, 1157.
6. Lynch, C. S., Fracture of ferroelectric and relaxor electroceramics: influence of electric field. *Acta Mater.*, 1998, **46**(2), 599–608.
7. Guiu, F., Hahn, B. S., Lee, H. L. and Reece, M. J., Growth of indentation cracks in poled and unpoled PZT. *J. Euro. Ceram. Soc.*, 1997, **17**, 505–512.
8. Park, E. T., Routbort, J. L., Li, Z. and Nash, P., Anisotropic microhardness in single-crystal and polycrystalline $BaTiO_3$. *J. Mat. Sci.*, 1998, **33**, 669–673.
9. Anstis, G. R., Chantikul, P., Lawn, B. R. and Marshall, D. B., A critical evaluation of indentation techniques for measuring fracture toughness: I. direct crack measurements. II. strength method. *J. Amer. Ceram. Soc.*, 1981, **64**, 533–539.
10. Lawn, B. R. and Marshall, D. B., Hardness, toughness and brittleness: an indentation analysis. *J. Amer. Ceram. Soc.*, 1979, **62**, 347–359.
11. Lawn, B. R., Evans, A. G. and Marshall, D. B., Elastic/plastic indentation damage in ceramics: the median/radial crack system. *J. Amer. Ceram. Soc.*, 1980, **63**(9–10), 574–581.
12. Lawn, B. and Wilshaw, R., Indentation fracture: principles and applications. *J. Mat. Sci.*, 1975, **10**, 1049–1081.
13. Meschke, F., Kolleck, A. and Schneider, G. A., R-curve behaviour of $BaTiO_3$ due to stress-induced ferroelastic domain switching. *J. Euro. Ceram. Soc.*, 1997, **17**, 1143–1149.
14. Schneider, G. A., Heyer, V. and Kolleck, A., Bruchmechanik ferroelektrischer Keramiken—Welche Wirkung hat ein elektrisches Feld? Deutscher Verband für Materialforschung und -prüfung e.V. DVM-Bericht 230, 1998, pp. 295–300.
15. Rice, R. W. and Pohanka, R. C., Grain-size dependence of spontaneous cracking in ceramics. *J. Am. Ceram. Soc.*, 1979, **61**(11,12), 559–563.
16. Suo, L., Mechanics concepts for failure in ferroelectric ceramics. *Smart Structures and Materials, ASME*, 1991, **AD24/AMD123**, 1–6.
17. McMeeking, R. M., Electrostrictive stresses near crack like flaws. *J. Appl. Math. Phys.*, 1989, **40**, 615–627.
18. Yang, W. and Suo, L., Cracking in ceramic actuators caused by electrostriction. *Journal of the Mechanics and Physics of Solids*, 1994, **42**(4), 649–663.
19. Suo, Z., Models for breakdown-resistant dielectric and ferroelectric ceramics. *Journal of the Mechanics and Physics of Solids*, 1993, **41**, 1155–1176.
20. Suo, Z., Kuo, C. M., Barnett, D.-M. and Willis, J. R., Fracture mechanics for piezoelectric ceramics. *Journal of the Mechanics and Physics of Solids*, 1992, **40**, 739–765.
21. Kittel, C., *Einführung in die Festkörperphysik*. R. Oldenbourg Verlag, München Wien, 1991.
22. Jackson, J. D., *Klassische Elektrodynamik*. Walter de Gruyter Berlin, New York, 1983.
23. Kreher, W. and Pompe, W., Increased fracture toughness of ceramics by energy-dissipative mechanisms. *J. Mat. Sci.*, 1981, **16**, 694–706.
24. Budiansky, B., Hutchinson, J. W. and Lambropoulos, J. C., Continuum theory of dilatant transformation toughening in ceramics. *Int. J. Solids Struct.*, 1983, **19**(4), 337–355.